

# European climatology of severe convective storm environmental parameters: A test for significant tornado events

Romualdo Romero <sup>a,\*</sup>, Miquel Gayà <sup>b</sup>, Charles A. Doswell III <sup>c</sup>

<sup>a</sup> *Departament de Física, Universitat de les Illes Balears, 07122 Palma de Mallorca, Spain*

<sup>b</sup> *Instituto Nacional de Meteorología, Centre Meteorològic a les Illes Balears, Palma de Mallorca, Spain*

<sup>c</sup> *Cooperative Institute for Mesoscale Meteorological Studies, Norman, OK, USA*

Accepted 22 June 2005

## Abstract

A climatology of various parameters associated with severe convective storms has been constructed for Europe. This involves using the reanalysis data base from ERA-40 for the period 1971–2000 and calculating monthly means, variability range and extremes occurrence of fields such as convective available potential energy, convective inhibition energy, mid-tropospheric lapse rate, low-tropospheric moisture content and storm relative helicity for different layers. This process is a first step towards development of a synthetic climatology of European severe weather, and is publicly available at the web site <http://ecss.uib.es>. Preliminary results derived from these products were presented during the ECSS 2004 conference. This paper is devoted to a more detailed presentation and discussion of the main results. It is hypothesized that preferred areas for severe thunderstorms occurrence in Europe would extend along a zonal belt over the south-central regions, where high helicity associated with the extratropical storm tracks and thermodynamically-favourable profiles established over the southern Atlantic and Mediterranean Sea would most likely be concatenated.

Further, this effort has been complemented with a collection of existing reports of significant (at least F2) tornadoes in Europe during the period 1971–2003. We present this data set in this paper and it also can be found at the website <http://ecss.uib.es>. Thus, the tornado collection can be used to test the appropriateness of the parameters selected for the synthetic climatology. In particular, it is found that the convective available potential energy, low-tropospheric moisture content and environmental shear, when related to the monthly climatology, are reasonably good descriptors of the tornadic environments.

© 2006 Elsevier B.V. All rights reserved.

*Keywords:* Europe; Climatology; Ingredients; Severe convection; Tornadoes

## 1. Motivation

A pan-European, self consistent and homogeneous database of severe convective reports is still a pending project, despite being an essential element for gaining

knowledge of the impact of severe convective storms in Europe and for the design of specific climatologies, forecasting methodologies and mitigation procedures. Unlike the US, where the National Weather Service has devoted resources for many years to a national compilation of severe weather reports, including tornadoes, convectively-induced severe winds and hail. Similar efforts in Europe have only been sporadic,

\* Corresponding author.

*E-mail address:* [Romu.Romero@uib.es](mailto:Romu.Romero@uib.es) (R. Romero).

not supported by national institutions and with a clear sub-regional focus (e.g. Gayà et al. (2001) for the Balearic Islands; Giaiotti et al. (2003) for north Italy; Leitão (2003) for Portugal; Marcinoniene (2003) for Lithuania, Setvák et al. (2003) for the Czech Republic; Sioutas (2003) for Greece; and Tyrrell (2003) for Ireland).

It should be mentioned here that a first step towards the development of a European Severe Weather report Database (ESWD) format has emerged from the last European Conferences on Severe Storms (see for details <http://www.essl.org/projects/ESWD>). The main challenges of this project include (a) to design a standardised universal code for the reports, (b) to channel the severe weather reports to a central point using the standardised format via Internet facilities, and (c) to articulate strategies for verification of the reports by weather professionals or trained persons. Apart from its own contribution to the construction of better climatologies, an important mission of the ESWD project is to assist in the skill assessment of routine forecasts explicitly aimed at the severe convective storm weather risks, an activity undertaken for the first time for Europe as a whole in the context of the recent initiatives: ESTOFEX (European Storm Forecast Experiment; <http://www.estofex.org>) and ESSL (European Severe Storms Laboratory, <http://www.essl.org>). However, the current content of the ESWD database is still too limited and geographically biased – with a much higher proportion of severe weather reports in Central European countries than in other areas – to permit the construction of reliable climatologies of severe convective storm occurrence over the whole of Europe.

Whereas the record of occurrence of severe convective storms in Europe is, and has been, somewhat erratic and sporadic, the real climatology of severe convection is likely to be more substantial than existing occurrence records would indicate. Thus, it is anticipated that by using an appropriate set of parameters that are recognized as relevant to severe convective storms, it should be possible to create a “synthetic climatology” of the occurrence frequencies by considering the time and space distributions of where these parameters become favourable for severe convective storms. The main objective of this paper is a first step in the construction of such synthetic descriptions of the real distribution of severe storms in Europe. Similar approaches (e.g. Brooks et al. 2003) have already shown the value of related parameters in discriminating between significant tornadic and non-tornadic thunderstorm environments in the United States, and how the regional climatologies of the

appropriate set of parameters can be used to infer the likelihood of severe convection occurrence in the data void regions of the world.

Moreover, by involving in the analysis a sufficiently large set of observed severe weather reports, it should be possible to test the appropriateness of the parameters selected for this synthetic climatology or, more precisely, to find the most useful parameters in a statistical sense. With this aim, we have developed a collection of significant tornadoes (at least F2 in the Fujita scale) that have been reported in Europe.

In Section 2, the meteorological data source that has been employed to perform both the synthetic climatology and the characterization of the significant tornado environments is presented. The selected dynamical and thermodynamic parameters are also indicated and the statistical products used to summarize the results are explained. In Section 3 the main results are presented and discussed, for the synthetic climatology and for the observed significant tornado events. It should be noted that the full content of this climatology is publicly available at <http://ecss.uib.es>. Finally, Section 4 is devoted to summarising the main conclusions and describing some future work necessary in order to improve this European climatology.

## 2. Meteorological data and statistical products

Proximity soundings are a tool used frequently to characterise the environmental conditions associated with the occurrence of convective storms. They form the basis of detailed analyses of case studies and have been used to elaborate specific climatologies over densely sampled continental areas (e.g. Brooks and Craven 2002; Doswell and Evans 2003). Except for their 12 h temporal spacing, routine rawinsoundings are an ideal dataset for this kind of studies in areas like central Europe, where the spatial density and homogeneity of the network is excellent. However, the spatial distribution of soundings is quite limited in peripheral areas of the continent, and important convective areas such as the Mediterranean basin are not well sampled. These restrictions, together with the need for efficient data handling, have motivated the use of the ERA-40 reanalysis dataset for our climatology, a recent development by the European Centre for Medium-range Weather Forecasts (ECMWF). Similar studies have already shown the value of this kind of reanalysed datasets for severe convective weather characterization (e.g. Brooks et al. 2003, which uses the NCAR/NCEP reanalysis system). In addition, Lee (2002) shows that proximity “pseudo-soundings” extracted from reanalysis

data can reproduce reasonably well the environmental conditions diagnosed from real proximity soundings, albeit with reduced vertical resolution.

The ECMWF ERA-40 dataset comprises 45-year (1957–2002) reanalysis of the global atmosphere and surface conditions. It has been built using observational datasets of many institutions, NCAR being the main supplier, exploiting the maximum information from observational sources and using an up-to-date data-assimilation system (see <http://www.ecmwf.int/research/era/Products> for details). The atmospheric data used in the study are available on standard pressure levels at six-hourly intervals (00, 06, 12 and 18 UTC) and with a grid spacing of about 125 km. The analyses of sea level pressure, geopotential height, temperature, relative humidity and horizontal wind were interpolated on a common limited area domain over Europe under a Lambert conformal map projection (see Fig. 1a), and then the analyses were used to calculate the following set of diagnostic variables (the coded name for each of

the variables which is going to be used as reference later in the text is indicated):

- convective available potential energy for the 1000 hPa “surface” parcel (CAPE, in  $\text{J kg}^{-1}$ )
- convective inhibition energy for the 1000 hPa “surface” parcel (CAPEN, in  $\text{J kg}^{-1}$ )
- mid-tropospheric (700–500 hPa) lapse rate (LR7050, in  $^{\circ}\text{C km}^{-1}$ )
- low-tropospheric (1000–850 hPa) moisture content, as measured by the precipitable water in that layer (PRWA85, in mm)
- deep layer (1000–350 hPa) storm relative helicity (SRH35, in  $\text{m}^2 \text{s}^{-2}$ )
- shallow layer (1000–850 hPa) storm relative helicity (SRH85, in  $\text{m}^2 \text{s}^{-2}$ )

where for SRH35 and SRH85, the storm motion was estimated applying the “30R75” rule on the mean wind of the layer 1000–400 hPa. That is, the storm motion is

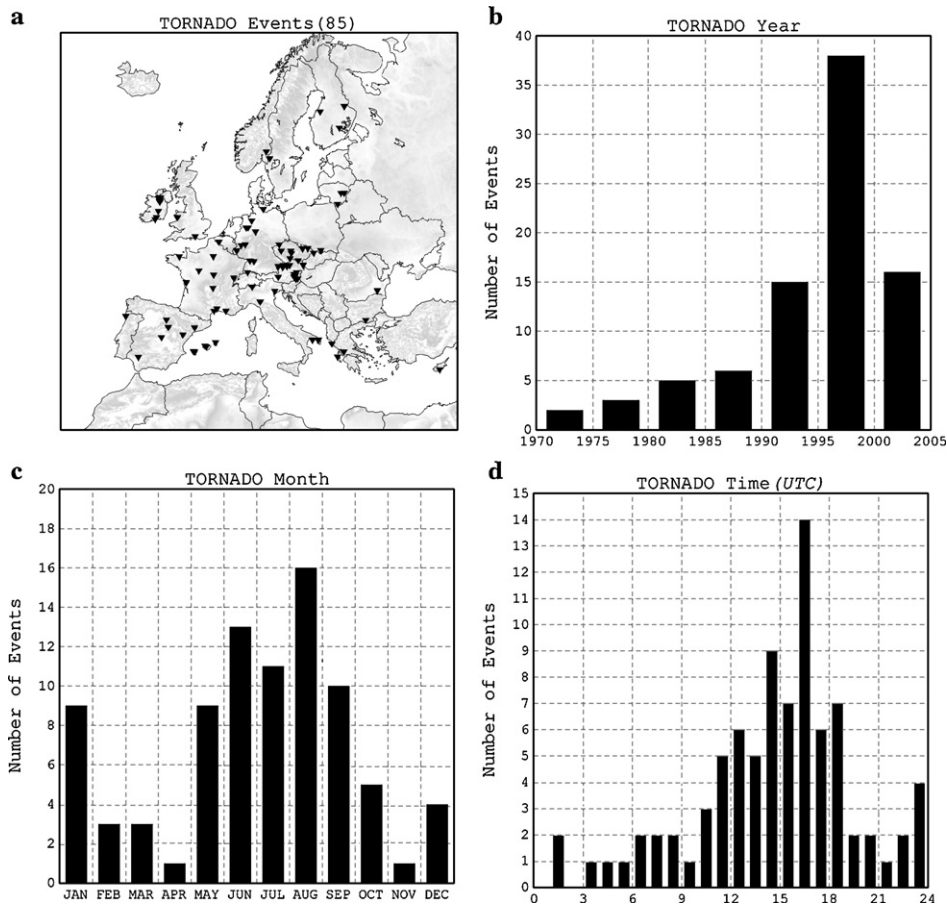


Fig. 1. Characteristics of the available collection of significant tornado events over Europe: a) Spatial distribution of the 85 events; b) yearly distribution; c) monthly distribution; and d) time distribution (time in UTC).

assumed to be  $30^\circ$  to the right of the mean wind and at 75% of the mean wind speed. Although there are many other dynamical and thermodynamic variables that could be considered to describe the convective environments, including a large collection of instability indices that appeared in the literature and different attributes of the parcel-theory derived cloud, only the previous six indicators have been considered at this early stage of the project. Even with such a small set, key basic ingredients that are associated with the development of severe thunderstorms (large values of convective and latent instability, high vertical shear and sufficient moisture at low-levels; Rasmussen and Blanchard, 1998) are included.

Furthermore, the following three additional variables were extracted from the reanalysis dataset in order to have a conventional picture of the prevailing synoptic pattern on the days with available tornado reports:

- geopotential height at 500 hPa (H500, in m)
- sea level pressure (SLP, in hPa)
- temperature field at 850 hPa (T850, in  $^\circ\text{C}$ ).

As noted in the last section, two types of statistical information were computed in the study. First, a climatology of each diagnostic variable for 1971–2000 at 12 UTC was created by computing monthly series of the following indicators:

- mean value (MEAN)
- 25% percentile value (QT25)
- 75% percentile value (QT75)
- inter-quartile range, that is, QT75–QT25 (IQR)
- number of days over threshold 1 (THRS1), 2 (THRS2), 3 (THRS3) and 4 (THRS4).

The fields QT25, QT75 and IQR serve to measure the spread of the population distributions for each month, whereas THRS1, THRS2, THRS3 and THRS4 are thresholds tailored for each of the diagnostic variables. These have been introduced to assess the occurrence of extremes. Specifically, these thresholds are 250, 500, 1000 and 2000  $\text{J kg}^{-1}$  for CAPE; 50, 100, 200 and 400  $\text{J kg}^{-1}$  for CAPEN; 6.5, 7.0, 7.5 and 8.0  $^\circ\text{C km}^{-1}$  for LR7050; 10, 12, 14 and 16 mm for PRWA85; 50, 100, 200 and 400  $\text{m}^2 \text{s}^{-2}$  for SRH35; and 25, 50, 100 and 200  $\text{m}^2 \text{s}^{-2}$  for SRH85. All these products can be graphically displayed as spatial distributions, since they were computed in each grid point over the considered European domain. Thus, a simple visual inspection of the resulting monthly maps allows a straightforward

qualitative and quantitative description of the different regional distributions in Europe across the year with respect to our selected environmental parameters associated with the genesis of severe convection.

Further, a collection of 85 significant – at least F2 estimated intensity – tornado events was identified according to trustworthy sources of information, such as our own database in the case of Spain and similar sources for other countries that were presented and published following past editions of the ECSS conference (Snow and Dessens 2001; Snow 2003). Most of these tornadoes are also included in the ESWD database. The spatial distribution of the 85 tornado events is quite irregular (Fig. 1a), showing wide areas over eastern and northern Europe and close to the Mediterranean with none or very few reports, whereas some regions of central Europe (notably Austria and the Czech Republic) have a very high number and density of reports. Rather than a true spatial distribution of the probability of having moderate/strong tornadoes, these results tend to reflect the great heterogeneity in tornado research and survey activity that is characteristic of European countries during the past. Consistently, the yearly distribution of the reports (Fig. 1b) tends to reflect the comparatively greater attention that the tornado problem has acquired in Europe during the last decade. In spite of the small number of tornadoes and the marked geographical heterogeneities, the resulting monthly and time distributions (Fig. 1c and d, respectively) appear to capture expected features of the tornadoes. For example, tornadic convection is more frequent during the warm season, owing to larger CAPE than during the cold season. Some tornadoes occur during winter in response to the regular incidence of active baroclinic disturbances (Fig. 1c). Further, most of the tornadoes occur during the afternoon hours in which the convective activity, at least over land surfaces, is also a maximum (Fig. 1d). A secondary maximum in tornado occurrence is observed around 24 UTC in Fig. 1d. Considering that underreporting is most likely during night hours, it can be hypothesized that this nocturnal relative maximum might be more substantial than what the relative signal appears to be.

For all the tornado events, a meteorological state was defined by searching the ERA-40 reanalysis dataset among the fields at 00, 06, 12 and 18 UTC on the day of the event for the first time prior to the tornado. For the few tornadoes after August 2002 (the ERA-40 ending time) operational grid analyses from the ECMWF were used instead. By computing the selected dynamical and thermodynamic variables at the tornado touchdown sites via interpolation from the surrounding grid points, it was

possible to locate the set of events within our selected parameter space and to compare their environments with the corresponding monthly climatology.

### 3. Results and discussion

#### 3.1. Synthetic climatology

##### 3.1.1. Convective available potential energy (CAPE)

The CAPE field follows a very well defined seasonal cycle over all European regions, being much larger during summer (maximum in July–August) than in the winter months (annual minimum reached in January–February). For instance, CAPE values in excess of 500 J kg<sup>-1</sup> are never observed on more than one day per month, on average, in January and February over all the European territory, whereas in July that threshold is reached for at least three days per month over most of the continent.

In reference to the transition seasons, higher CAPE values are found in autumn than spring in the Mediterranean environment, that is, over the Mediterra-

nean Sea and neighbouring coastal counties. This is expected, because after the high summer insolation, the Mediterranean Sea remains warm for several weeks following the peak insolation and acts as a powerful heat and moisture source. However, farther north, over continental Europe, that character of the CAPE annual cycle is reversed; that is, May and June exhibit higher CAPE values than September and October. This implies that in much of continental Europe, diurnal surface heating occurring beneath relatively cool air masses aloft appears to be the most important factor.

Regardless of the specific values observed, which are much lower outside the summer months, the general pattern of the CAPE distribution shown in Fig. 2 is a quasi-permanent feature during the full year. The Mediterranean clearly exerts a dominating influence on the CAPE distribution pattern. Its influence is not limited to directly over the sea but is noted over the southern Europe countries, very much like the role played by the Gulf of Mexico waters for the southern plains of United States. Regions with the largest CAPE values (darker areas in Fig. 2a), generally correspond

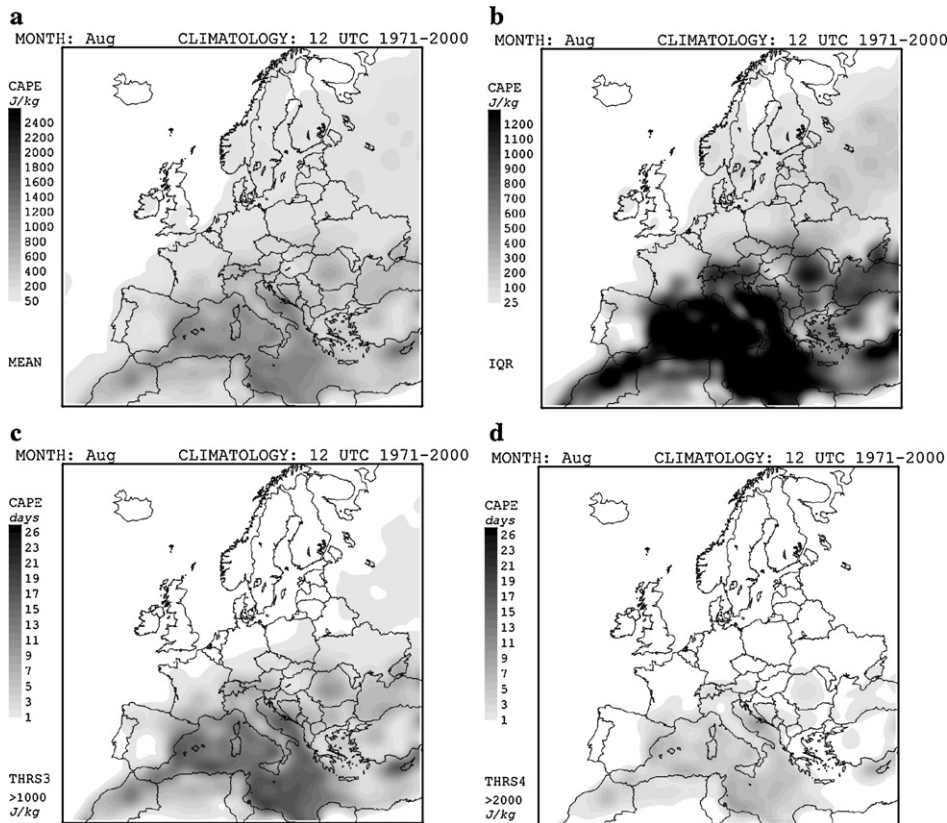


Fig. 2. Monthly climatology of CAPE for August, showing: a) mean value (MEAN); b) inter-quartile range (IQR); c) number of days above 1000 J/kg (THRS3); and d) number of days above 2000 J/kg (THRS4). Note the units and scale on the left of each map.

with the highest day to day variability as measured by the IQR index (Fig. 2b). CAPE values as high as  $1000 \text{ J kg}^{-1}$  are typically observed on several days during the summer months over the southern half of Europe (Fig. 2c). However, very high CAPE values ( $2000 \text{ J kg}^{-1}$  and larger) are limited primarily to the Mediterranean and Black Seas and neighbouring regions affected in an average month (see Fig. 2d).

### 3.1.2. Convective inhibition energy (CAPEN)

This field exhibits a similar seasonal cycle to CAPE (maximum in summer and minimum in winter), but the differences between the opposite seasons are not as obvious. In all seasons, the largest CAPEN values are found toward the south of the domain, with the spatial differences stronger in summer than in winter. The characteristic spatial distribution of CAPEN-related indices can be appreciated on Fig. 3, which again corresponds to August. The most interesting feature is that the high-CAPE prone Mediterranean environment also shows high values of convective inhibition (Fig. 3a). This inhibition is typically greater towards the

western Mediterranean (around Iberia–Morocco–Algeria) and eastern Mediterranean (around Turkey and Cyprus) than in its central part (that is, around Italy). This is probably a reflection of the frequent overrunning of the low-level Mediterranean moist air by well mixed layers originating in the dry, elevated terrain of Africa, the Iberian Peninsula and Turkey, very much like the role exerted by the Mexican plateau for the US southwestern plains (Carlson and Ludlam 1968). In fact, the greatest CAPEN values are found off the coast of Morocco over the Atlantic, where in contrast, CAPE values are typically small (recall Fig. 2a) owing to sparse low-level moisture. It is interesting to note that wide oceanic Atlantic areas combine appreciable CAPEN signatures with very small – or infrequent – CAPE values (compare Figs. 3a and 2a, respectively), emphasizing the unfavourable conditions for deep convective developments in those areas on the average. On the other hand, the variability in the CAPEN values is the highest around the Mediterranean (Fig. 3b) and, when looking at the number of occasions in which high inhibition energies are reached (Fig. 3c and d), the

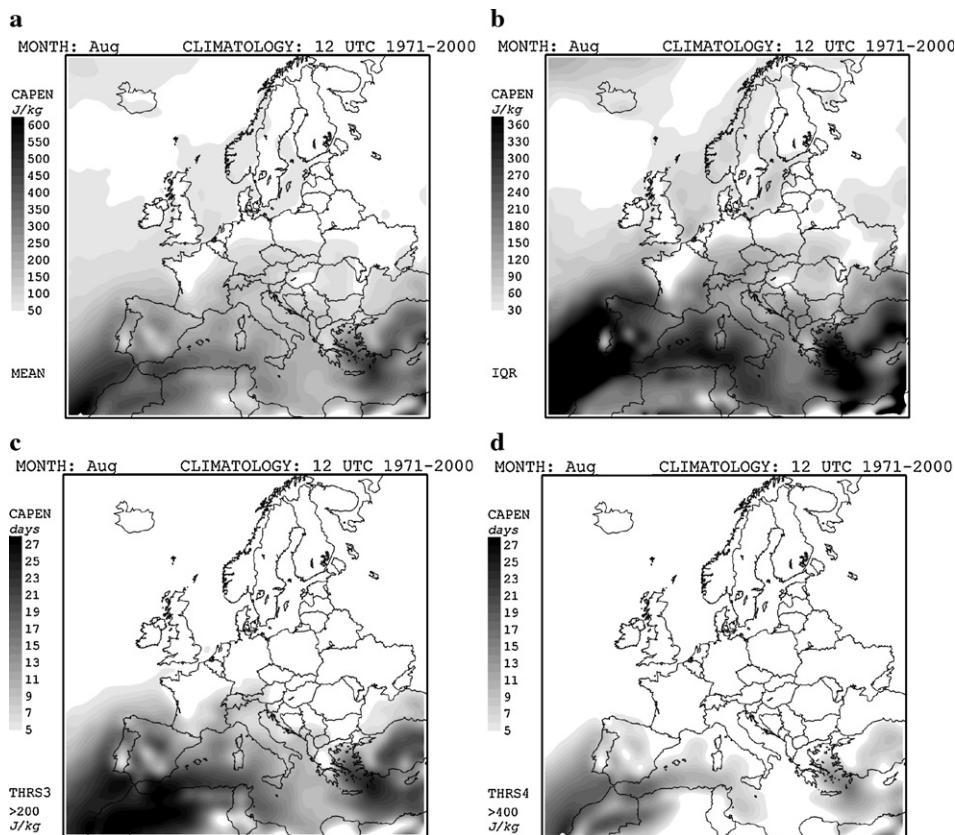


Fig. 3. Monthly climatology of CAPEN for August, showing: a) mean value (MEAN); b) inter-quartile range (IQR); c) number of days above  $200 \text{ J/kg}$  (THRS3); and d) number of days above  $400 \text{ J/kg}$  (THRS4). Note the units and scale on the left of each map.

forementioned positive signals about Iberia–Morocco and Turkey–Cyprus are still more evident.

3.1.3. Mid-tropospheric lapse rate (LR7050)

The lapse rate between 700 and 500 hPa is included in the study to reflect the thermal contribution to the convective destabilization of the troposphere, although the dominant role in creating moist convective atmospheres generally belongs to the low-level humidity rather than to the lapse rate. The seasonal contrast of the LR7050 field is well illustrated in Fig. 4, which shows MEAN and IQR for January and July. In winter, average LR7050 values are quite uniform over the continent but the highest lapse rates are found along the eastern Atlantic and the Mediterranean (Fig. 4a). This signature appears to be associated with the high frequency of baroclinic cyclones that affect both regions. Orography – particularly the Atlas Mountains and the Alps for the Mediterranean – clearly plays an important role in this structure. When considering the daily variability of lapse rates (Fig. 4b), there is a high contrast in the values between the high latitude Atlantic areas and the rest of

the domain. The high variability in the former areas is likely to be a consequence of the intense transient disturbances that affect the region during the cold season. In the rest of the domain, the variability is much less and spatially very uniform.

During summer, characteristic lapse rates are low over most of Europe, apparently due to the infrequency of deep synoptic disturbances, but this is reversed over Africa, Iberia and the western Mediterranean, where lapse rates increase significantly (Fig. 4c). Relatively high values are also found along the coastal lands north of the Mediterranean, especially in Turkey. This highlights the effect of the strong surface heating occurring during summer in the elevated terrain of those regions on the lapse rate, as noted previously when discussing the CAPEN field. The highest daily variability of LR7050 is found in extreme northern Africa and northward from there, especially over the Atlantic sector of Morocco and over the western Mediterranean and southeastern Spain (Fig. 4d), precisely in the same areas where large convective inhibition energies were noted in Fig. 3. The high variability of LR7050 in those

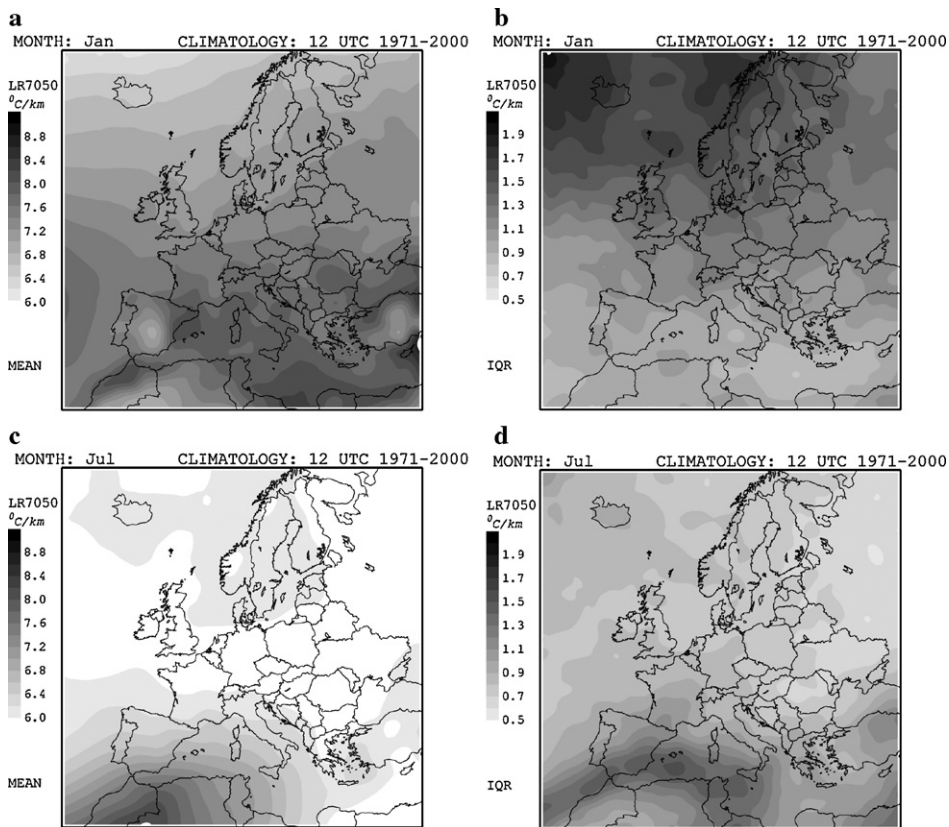


Fig. 4. Monthly climatology of LR7050, showing: a) mean value (MEAN) and b) inter-quartile range (IQR) for January; c) mean value (MEAN) and d) inter-quartile range (IQR) for July. Note the units and scale on the left of each map.

areas appears to respond to the episodic nature of the African air intrusions that regularly affect those areas during the summer.

Similar maps for the other two seasons reveal higher lapse rates in spring than in autumn, a logical consequence of the increased surface warming acting on the characteristic spring-time cool air masses at low-levels, as well as the transport of heat into the middle and upper troposphere by summertime convection (see [Doswell and Bosart 2001](#)). Generally a southward increase of the average LR7050 values (maps not shown) is found.

### 3.1.4. Low-tropospheric moisture content (PRWA85)

Low-level moisture is a primary ingredient in convective environments. For Europe, the main moisture sources are the Mediterranean Sea to the south and the Atlantic Ocean to the west. The Mediterranean is relatively warm even in winter and this explains its great evaporative potential throughout the year. The Atlantic exhibits high sea surface temperatures only in its southern sector; that is, roughly at the latitudes of the

Iberian Peninsula. Accordingly, average low-level moisture contents in Europe increase southward and the maximum values are found over the Mediterranean and west of the Iberian Peninsula and Morocco over the Atlantic. Such a southward gradient is a permanent feature in all seasons, but the available moisture is obviously greater during the warm season owing to higher sea surface temperatures. In fact, low-level moisture content is greatest in summer, followed by autumn, spring and winter in agreement with the sea surface temperature evolution.

As a clear example of the spatial distribution of PRWA85, [Fig. 5](#) shows some of the maps corresponding to August. It can be observed that large values of low-level moisture are spread from the Mediterranean and the southern Atlantic into wide regions of southern Europe, with values gradually diminishing toward Scandinavia and the northern Atlantic ([Fig. 5a](#)). It is interesting to note that the PRWA85 variability is higher over land than over the oceanic areas ([Fig. 5b](#)). This appears to be a logical consequence of the fact that the moisture content of air masses lying over water is

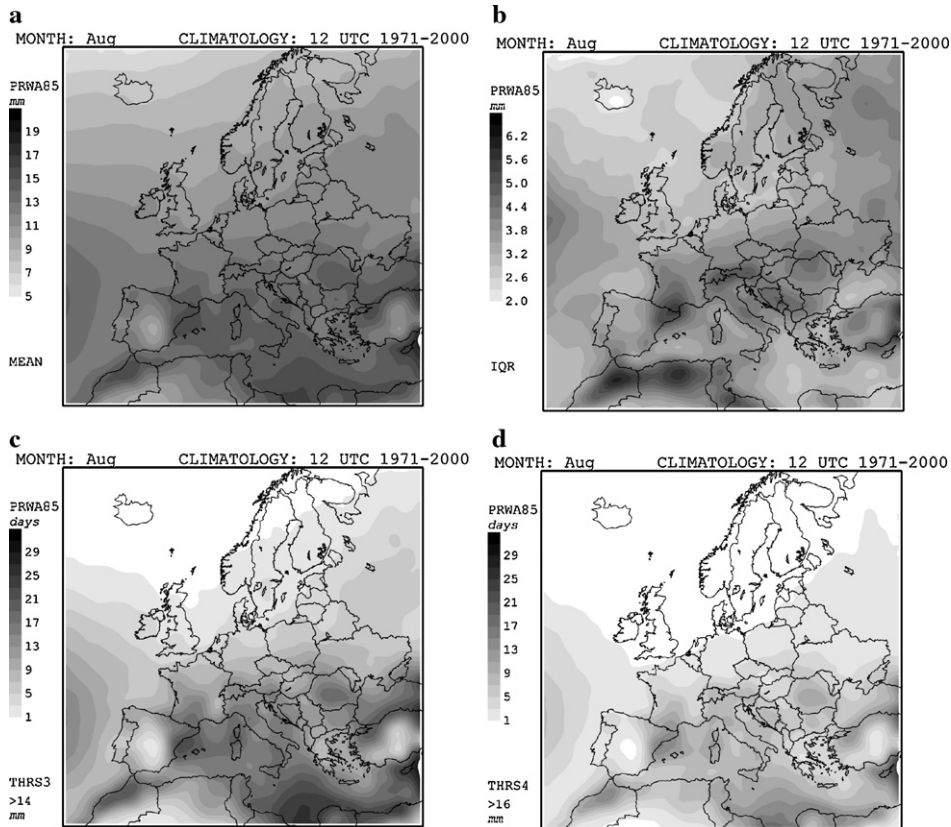


Fig. 5. Monthly climatology of PRWA85 for August, showing: a) mean value (MEAN); b) inter-quartile range (IQR); c) number of days above 14 mm (THRS3); and d) number of days above 16 mm (THRS4). Note the units and scale on the left of each map.

relatively constant, whereas over land the moisture variable is more irregular in response to the changing flow direction (maritime or continental). When the PRWA85 is analysed in terms of the number of days a given threshold is exceeded, high moisture contents are frequently reached over the Mediterranean and southern Atlantic and many continental areas of southern Europe (Fig. 5c and d). The exceedance frequencies are obviously much lower outside the warm season (not shown).

3.1.5. Deep layer storm relative helicity (SRH35)

Vertical shear of the horizontal wind through the troposphere is strongly influenced by the baroclinicity of the environment, as a result of the wind above the boundary layer being dominated by the geostrophic component. The largest values are found in association with the passage of extratropical cyclones, which are more frequent and deeper during the cold season. In winter (Fig. 6a) the average helicity is about twice the average value of the summer (Fig. 6c), at least over large parts of mid- and high latitudes of Europe. In southern

Europe, approaching the African continent, the differences between winter and summer are not so marked. Intermediate values of SRH35 are found in the other two seasons (spring and autumn), but while in central and northern latitudes helicity is higher in autumn than spring, in the southern part of the domain it is higher in spring (maps not shown).

An interesting – and expected – aspect of the storm-relative helicity field observed in all months is the absolute maximum located over the Atlantic at the latitude of Great Britain (Fig. 6a and c). This signature clearly reflects the north Atlantic storm track. It should be noted that relatively high values of helicity are not confined to the Atlantic Ocean but also affect wide areas of Atlantic and Central Europe, especially in winter. The variability of the SRH35 field (Fig. 6b and d) basically mimics the mean field, so that the largest values are found in association with the typical paths of the baroclinic storms at mid-high latitudes. It is interesting to note that IQR is relatively high during summer over the western Mediterranean (Fig. 6d) but it is the minimum of the domain during winter (Fig. 6b).

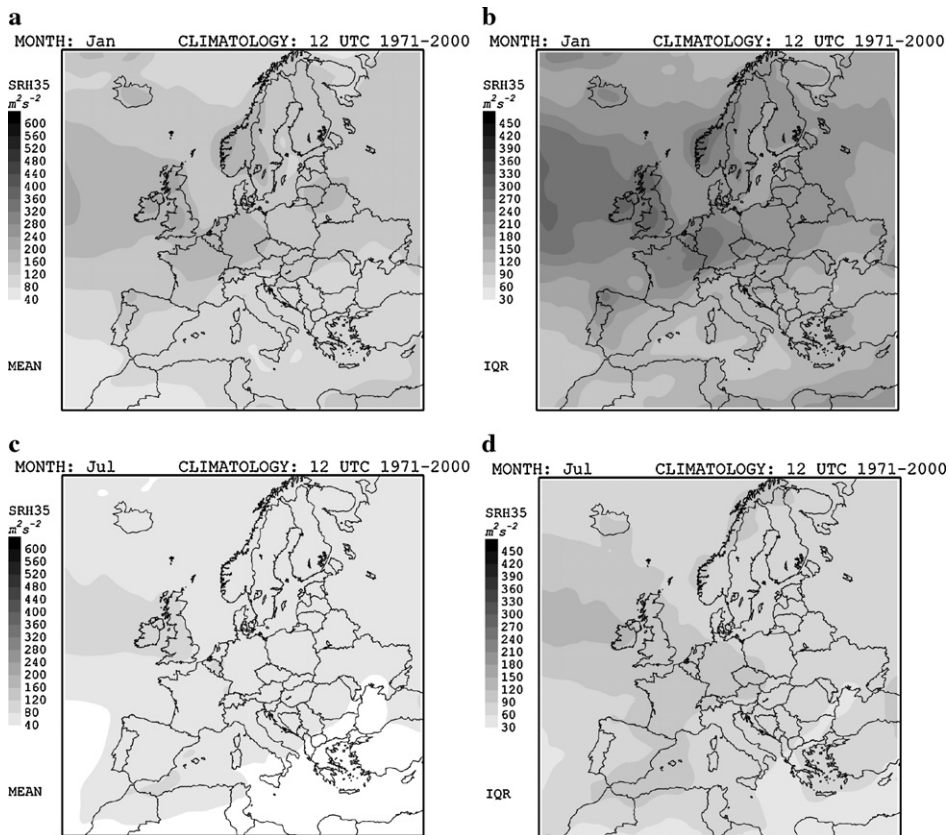


Fig. 6. Monthly climatology of SRH35, showing: a) mean value (MEAN) and b) inter-quartile range (IQR) for January; c) mean value (MEAN) and d) inter-quartile range (IQR) for July. Note the units and scale on the left of each map.

### 3.1.6. Near-surface layer storm relative helicity (SRH85)

As SRH85 is diagnostic of the vertical shear in a relatively shallow layer near the surface, it is much more influenced by topography and boundary layer effects than the deep layer shear. Substantial contrasts for this field are seen between oceanic and land areas. In any season, characteristically greater near-surface storm relative helicity is found over the continent and islands than over adjacent waters, owing to the enhanced directional shear imposed by the greater friction over land (see Fig. 7a and c, corresponding to January and July, respectively). Although deep layer shear is strongly influenced by baroclinicity through the geostrophic contribution to shear, the near-surface shear is strongly affected by ageostrophic factors that may not necessarily be represented well in the assimilated fields used by numerical models. Apart from the notable sea–land contrasts, the SRH85 field exhibits some of the behaviours already noted for SRH35: larger values in winter than in summer and intermediate values in the transition seasons, with spring and autumn yielding higher helicity in the south and the centre-north,

respectively; increasing helicity towards the north–northwest but with a less clear signature in this case of the Atlantic storm track; and greater variability among the SRH85 daily values over central and northern Europe and the Atlantic ocean than in other areas (see Fig. 7b and d, respectively, for IQR in January and July).

### 3.2. Significant tornado events

In spite of the limitations of the current events database – a small sample with only 85 cases and geographically biased – a statistical comparison of the above environmental parameters calculated for the approximate time and location of the tornado touch-down points (as discussed previously) with the corresponding monthly climatologies could provide some preliminary assessment of which variables are most useful for describing the environments associated with the genesis of tornadic thunderstorms in Europe. For that purpose, we present for each variable the frequency distribution of the collection of cases both in terms of the attained value of the parameter and in terms of the corresponding percentile when comparing with

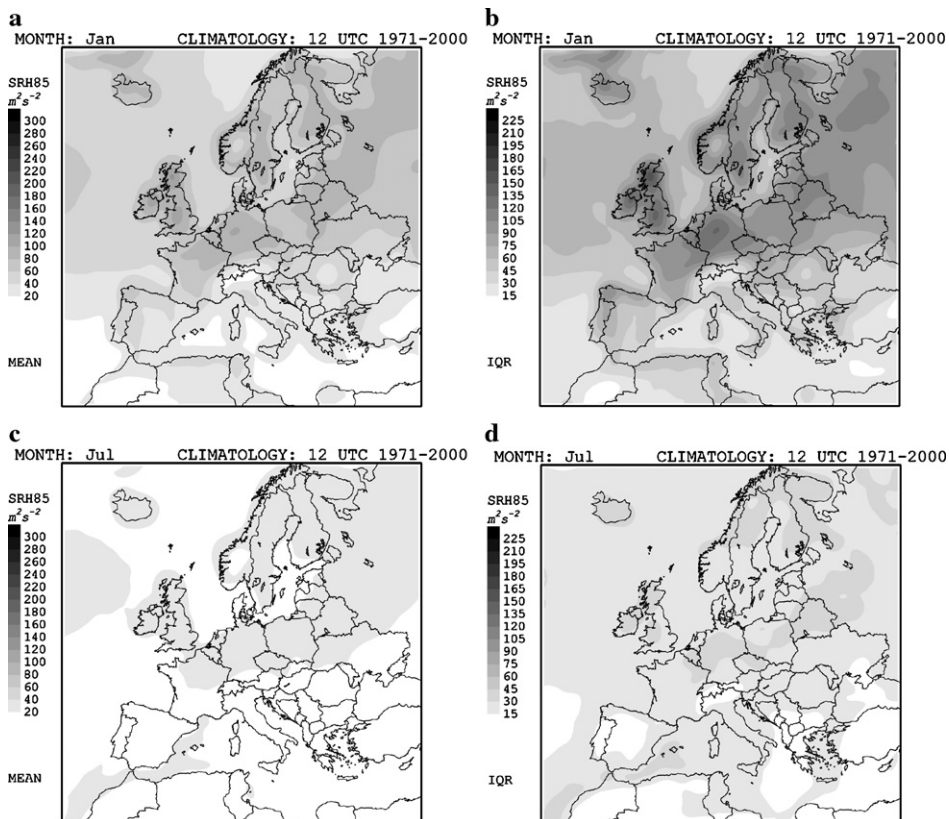


Fig. 7. Monthly climatology of SRH85, showing: a) mean value (MEAN) and b) inter-quartile range (IQR) for January; c) mean value (MEAN) and d) inter-quartile range (IQR) for July. Note the units and scale on the left of each map.

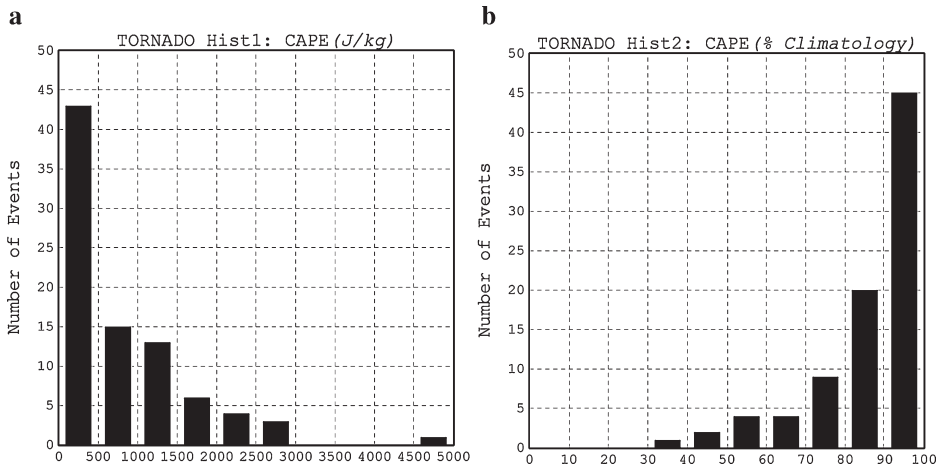


Fig. 8. Frequency distributions for the significant tornado events as function of: a) CAPE value; b) Percentile of the corresponding monthly climatology of CAPE. Units of the horizontal axis are J/ kg and % in a) and b), respectively.

the daily values that define the 1971–2000 climatology for its month.

3.2.1. Convective available potential energy (CAPE)

In terms of the CAPE parameter, most of the tornadoes occurred in environments with weak to moderate instability (less than 500 J kg<sup>-1</sup> for half of the tornadoes; see Fig. 8a), although a few of them occurred with very large values of CAPE (up to 4500–5000 J kg<sup>-1</sup> for one of the cases). What is revealing is to compare the conditions existing at the time and location of the event with the local climatology (Fig. 8b). It is observed that most of the tornadoes occurred in environments with abnormally high CAPE values, such that 45 of the tornadoes occurred in an environ-

ment beyond the 90% percentile of the CAPE distribution for its month.

3.2.2. Convective inhibition energy (CAPEN)

Associated with the occurrence of significant tornado events, convective inhibitions tend to be rather small in absolute terms (50 events exhibited less than 50 J kg<sup>-1</sup>; Fig. 9a). When comparing with the monthly climatology, however, a flat distribution is found, with no clear dominance of any percentile range (Fig. 9b). Therefore, the CAPEN anomaly with respect to the climatology seems to be a rather poor discriminating factor for the tornado likelihood. It should be noted that the reanalysis data, owing to its poor vertical resolution, could be compromising this result. It is also known that some

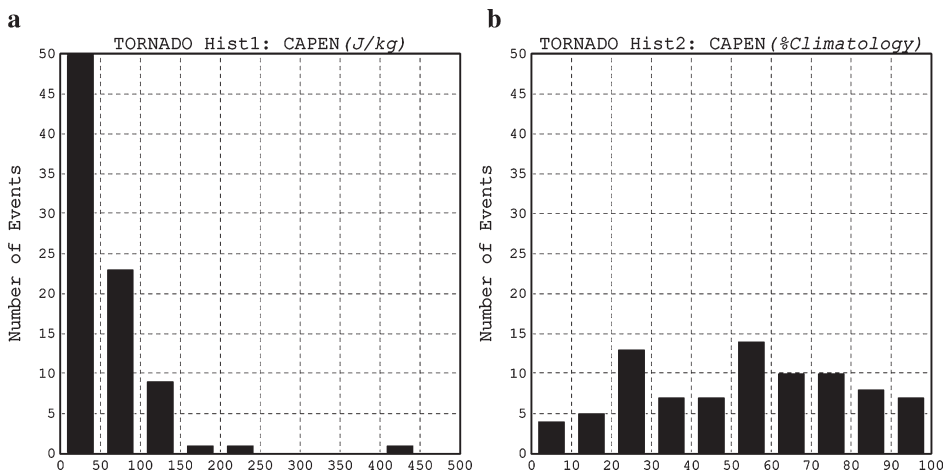


Fig. 9. Frequency distributions for the significant tornado events as function of: a) CAPEN value; b) percentile of the corresponding monthly climatology of CAPEN. Units of the horizontal axis are J/ kg and % in a) and b), respectively.

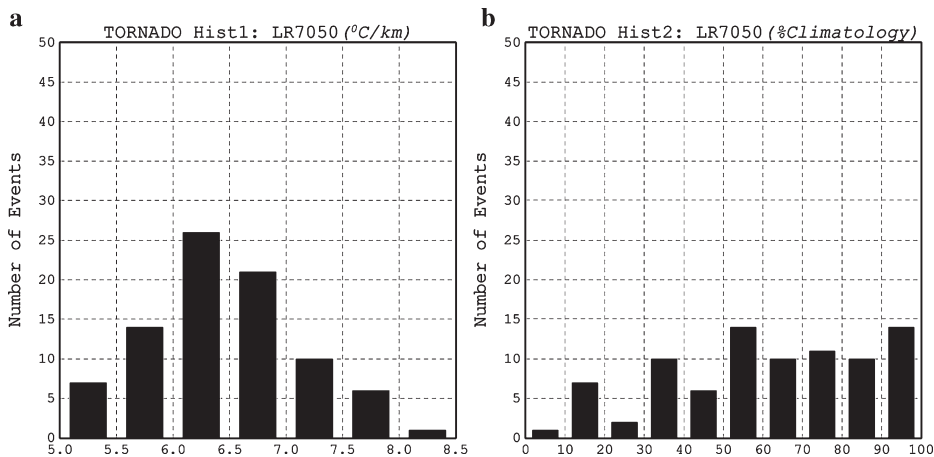


Fig. 10. Frequency distributions for the significant tornado events as function of: a) LR7050 value; b) percentile of the corresponding monthly climatology of LR7050. Units of the horizontal axis are °C/km and % in a) and b), respectively.

convective inhibition can be favourable for tornadoes, but too much inhibition prevents convection from developing at all. There is some weak indication of this in Fig. 9b, given that the peak in the generally flat distribution is near the median value, although it is not a strong result of this analysis.

### 3.2.3. Mid-tropospheric lapse rate (LR7050)

The frequency distribution of the mid-tropospheric lapse rates exhibits a central maximum around the standard atmospheric value of  $6.5 \text{ °C km}^{-1}$  (Fig. 10a). In reference to the climatology, Fig. 10b shows a certain tendency for above than average lapse rates in the tornado environments, but Fig. 10b suggests that LR7050 by itself is not an appropriate discriminating variable, as could be expected.

### 3.2.4. Low-tropospheric moisture content (PRWA85)

In contrast with the two previous parameters, the low-tropospheric moisture content is a dominant variable for the diagnosis of tornado occurrence. The distribution of PRWA85 values is not very indicative of the appropriateness of this index since a wide range of values is found among the 85 tornadoes (most of them in the 10–20 mm interval; Fig. 11a), but when these values are considered according to the monthly climatology, a very skewed distribution emerges (Fig. 11b). The great majority of the events exhibited high (above the 80% percentile) PRWA85 contents and practically half of them lie in the 90–100% class. Clearly, then, as expected, the presence of very moist air in the lower troposphere appears to be a necessary ingredient for the genesis of tornadic thunderstorms.

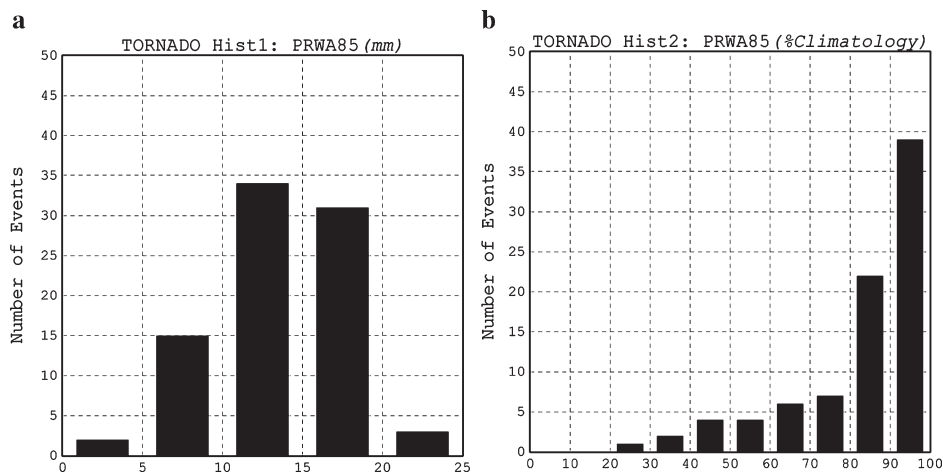


Fig. 11. Frequency distributions for the significant tornado events as function of: a) PRWA85 value; b) percentile of the corresponding monthly climatology of PRWA85. Units of the horizontal axis are mm and % in a) and b), respectively.

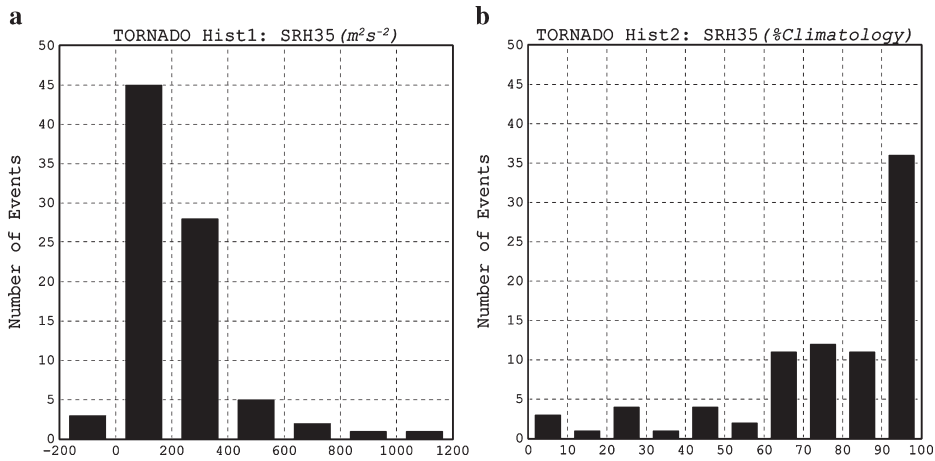


Fig. 12. Frequency distributions for the significant tornado events as function of: a) SRH35 value; b) percentile of the corresponding monthly climatology of SRH35. Units of the horizontal axis are  $m^2 s^{-2}$  and % in a) and b), respectively.

### 3.2.5. Deep layer storm relative helicity (SRH35)

Another influencing parameter for tornadogenesis is the deep layer vertical shear (Fig. 12), in agreement with the conceptual/theoretical models of supercell environments and the observations in other locations, like the US. When considered in absolute terms, however, SRH35 does not appear as a very critical variable, since most of the tornado events exhibited less than  $400 m^2 s^{-2}$  (Fig. 12a), but again in comparison with the climatology the majority presented quite significant storm relative helicity and as many as 36 of them occurred in environments above the 90% percentile (Fig. 12b).

### 3.2.6. Near-surface storm relative helicity (SRH85)

A very similar picture to the previous one is found when using as a parameter the SRH in a shallow layer.

Again, the absolute values of the variable by itself seem not to be very useful as a discriminating factor, in the sense that the helicity for most of the tornado events was rather low (Fig. 13a), but again, compared with the monthly climatology, it is observed that many of the tornadoes occurred with relatively high values of SRH85 (Fig. 13b). Comparing Figs. 12b and 13b, it can be hypothesized that SRH85 is a slightly better discriminating parameter than SRH35. This is consistent with Hanstrum et al. (2002) and Monteverdi et al. (2003), who found that the 0–1 km shear could be an effective tornado forecast variable, in combination with others.

### 3.2.7. Other variables (H500, SLP and T850)

As was noted in Section 2, we also considered some indicators of the synoptic setting when analysing the

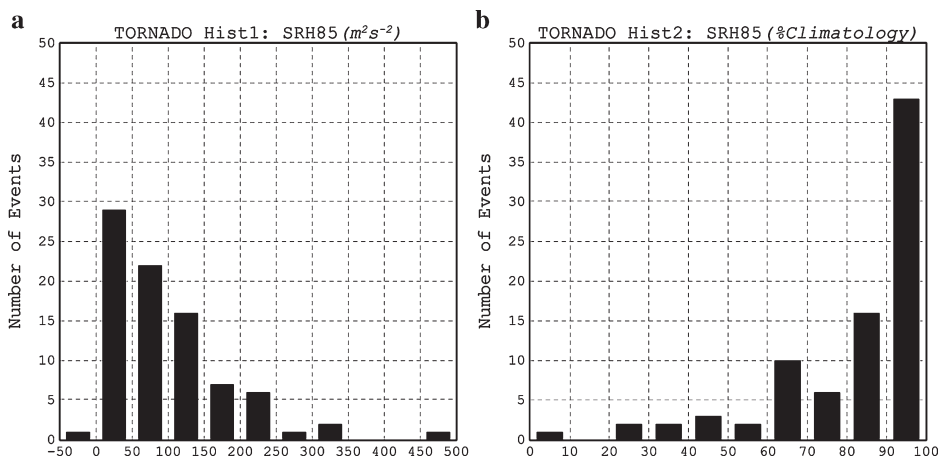


Fig. 13. Frequency distributions for the significant tornado events as function of: a) SRH85 value; b) percentile of the corresponding monthly climatology of SRH85. Units of the horizontal axis are  $m^2 s^{-2}$  and % in a) and b), respectively.

tornado events: geopotential height at 500 hPa (H500), sea level pressure (SLP) and temperature at 850 hPa (T850). As was done for the other thermodynamic variables, we compared the local values at the time and place of the events with the corresponding monthly climatology (Fig. 14). In fact, Fig. 14 does not provide complete information about the synoptic circulation pattern prevailing at the time of the event, since it is only based on a point value for the variables. However, it permits an analysis of the tornadic environments in terms of the possible anomalies of the height, pressure and temperature fields, an aspect which could well be of interest.

In the first place, a quite uniform distribution of the H500 percentile classes (Fig. 14a) is found, although with slightly higher occurrences of low geopotential heights, that is, under the likely nearby presence of troughs or cut-offs in the middle troposphere. Much more clear indications are found in the sea level

pressure field, such that half of the events presented SLP values below the 10% percentile of the corresponding monthly climatology. Stated differently, the presence of a surface depression in the vicinity of the severe convective area can be considered an important feature in the tornado environment. Finally, most of the tornadic thunderstorms occurred in relatively warm air masses at low-levels (Fig. 14c), a not unexpected result, given what we have already seen from the other variables.

#### 4. Conclusions and future work

A climatology of selected severe convective environmental variables has been constructed for Europe, where a very little exists in the way of systematic and funded efforts to compile and verify severe weather reports. This climatology, available at <http://ecss.uib.es>, has been conceived as a synthetic piece of information

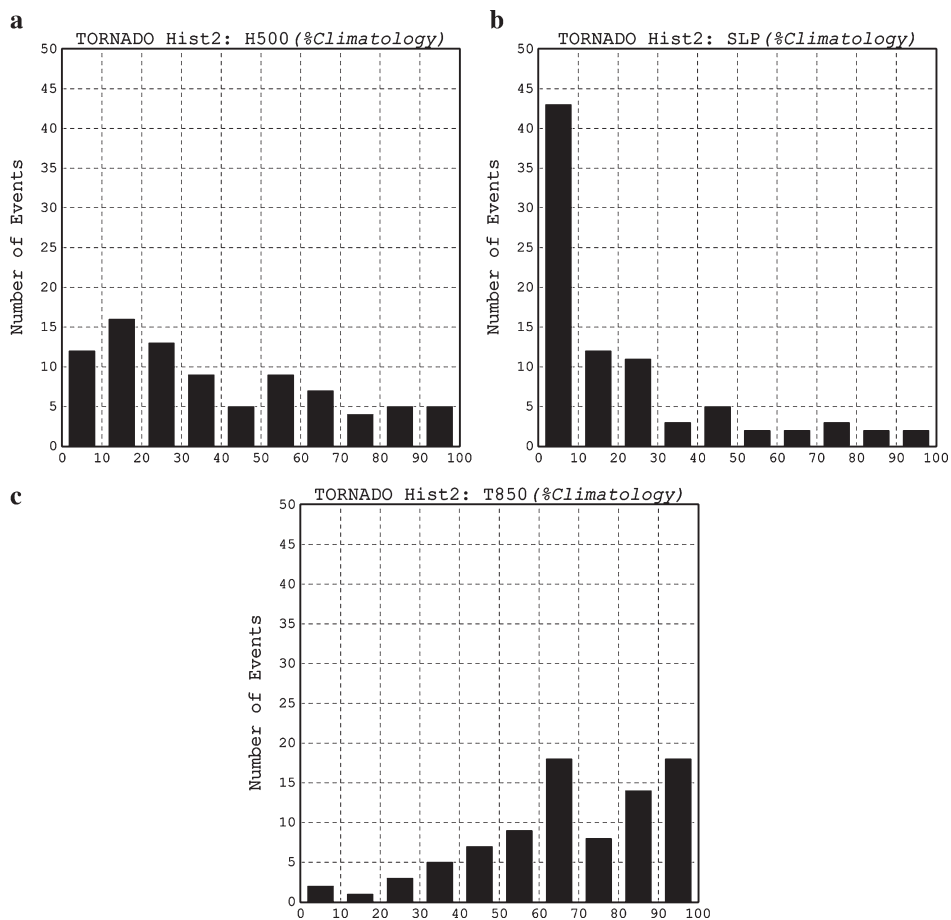


Fig. 14. Frequency distributions for the significant tornado events as function of the percentile of the corresponding monthly climatology of the variables: a) H500; b) SLP; and c) T850. Units of the horizontal axis in a), b) and c) are %.

useful to define, to a first approximation, the main areas where and when recognized severe convective ingredients frequently are found. The climatology is based on the ERA40 reanalysis dataset (grid resolution 125 km) and uses monthly statistical indexes, so very local or transient features have been sacrificed in our analysis in favour of a rather general description of the problem for the full European continent and other contiguous areas such as the northern Atlantic, the Mediterranean Sea and north Africa. On the other hand, only a few of the myriad possible environmental variables have been considered at this first stage of the project: convective available potential energy, convective inhibition energy, mid-tropospheric lapse rate, low-tropospheric moisture content and both deep and shallow layer storm relative helicity.

Although most of our results could have been qualitatively expected, we have developed quantitative assessments, allowing us to depict some interesting patterns evolving in the European domain during the year. It is plausible to make a clear distinction between the considered thermodynamic ingredients (particularly convective instability and low-tropospheric moisture content) and the dynamical ingredients (shallow and deep layer storm relative helicity). The former increase southward, as they are basically built over the warm waters of the southern Atlantic and the Mediterranean, whereas the later increase northward, since they are strongly regulated by the incidence of synoptic-scale disturbances that are more frequent along the well defined Atlantic and Western Europe extratropical cyclone tracks. If we follow the well established conceptual model that tornadic severe weather from supercell thunderstorms requires a combination of significant values of both static instability and shear, we can conclude that favourable environments for tornadic convection in Europe would be most likely along a latitudinal belt covering the south-central countries of the continent. This hypothesis is essentially derived from the monthly maps analysed in the study, which exhibited in those zones moderate values of the average dynamical and thermodynamic parameters and also a significant variability, a reflection of the episodic nature of the meridional incursions of the tornado-favourable environmental ingredients in the mid-latitudes.

Further, a collection of 85 trustworthy tornado reports in the F2+ category were compiled to assist in this study. Specifically, the reports have been used to test the appropriateness of the parameters selected for the synthetic climatology. Particularly interesting was the relative capability of the selected variables for sepa-

rately characterising significant tornado environments. Convective available potential energy, low-tropospheric moisture content and environmental shear were all found quite useful for that purpose, but only when they were expressed in relation to the monthly climatological values. That is, they become useful indicators of the likelihood for tornadoes when the monthly climatological mean is substantially exceeded, regardless of the absolute value that is attained. Obviously, these findings are preliminary until we involve in the statistical analysis a good number of nontornadic thunderstorm events. Moreover, with an increasing number of tornado reports, it would be interesting to focus the statistical analysis as function of tornado intensity or other attributes.

Another pending work in this European climatology is the inclusion of other severe convective weather events, basically hail and convectively-induced severe wind reports. We are very interested in flash flood events as well, the impact of which is very important in areas like Mediterranean Europe. Obviously, a sufficient sample of events for each category (well beyond the 85 cases used in this study) must be included to produce reliable statistics and a rigorous intercomparison of the results. In this sense, the existing interactions between the authors and the recently articulated European Severe Weather report Database (ESWD Project) should be fruitful and beneficial for the completion and improvement of our climatology.

Finally, other physically-based and empirical convective indices that are used in severe convective storm forecasting will be added to our list of parameters in order to widen the potential of this European climatology of severe storms.

## Acknowledgements

This research was stimulated and initiated while the third author, Charles A. Doswell III, enjoyed a sabbatical stay at UIB under project SAB2002-0084 of the Spanish Ministerio de Educación, Cultura y Deportes. Financial support by the same institution through the MEDEXIB project (REN2002-03482/CLI) is also acknowledged. Our PhD student Lluís Fita is sincerely acknowledged for his great effort in archiving the ERA-40 dataset used for the study, as it is our web designer Noelia Ferragut for constructing and maintaining the associated web site <http://ecss.uib.es>. Finally, we wish to remember that ERA-40 is a project hosted by the European Centre for Medium-Range Weather Forecasts (ECMWF).

## References

- Brooks, H.E., Craven, J.P., 2002. A database of proximity soundings for significant severe thunderstorms, 1957–1993. Preprints, 21st Conference on Severe Local Storms, San Antonio, Texas, Amer. Meteorol. Soc, pp. 639–642.
- Brooks, H.E., Lee, J.W., Craven, J.P., 2003. The spatial distribution of severe thunderstorm and tornado environments from global reanalysis data. *Atmos. Res.* 67–68, 73–94.
- Carlson, T.N., Ludlam, F.H., 1968. Conditions for the occurrence of severe local storms. *Tellus* 20, 203–226.
- Doswell III, C.A., Bosart, L.F., 2001. Extratropical synoptic-scale processes and severe convection. *Severe Convective Storms. Meteorol. Monogr. Am. Meteorol. Soc.* 28 (50), 27–69.
- Doswell III, C.A., Evans, J.S., 2003. Proximity sounding analysis for derechos and supercells: an assessment of similarities and differences. *Atmos. Res.* 67–68, 117–133.
- Gayà, M., Homar, V., Romero, R., Ramis, C., 2001. Tornadoes and waterspouts in the Balearic Islands: phenomena and environment characterization. *Atmos. Res.* 56, 253–267.
- Giaiotti, D., Nordio, S., Stel, F., 2003. The climatology of hail in the plain of Friuli Venezia Giulia. *Atmos. Res.* 67–68, 247–259.
- Hanstrum, B.N., Mills, G.A., Watson, A., Monteverdi, J.P., Doswell III, C.A., 2002. The cool-season tornadoes of California and Southern Australia. *Weather Forecast.* 17, 705–722.
- Lee, J.W., 2002. Tornado proximity soundings from the NCEP/NCAR reanalysis data. MS Thesis, University of Oklahoma, 61 pp.
- Leitão, P., 2003. Tornadoes in Portugal. *Atmos. Res.* 67–68, 381–390.
- Marcinioniene, I., 2003. Tornadoes in Lithuania in the period of 1950–2002 including analysis of the strongest tornado of 29 May 1981. *Atmos. Res.* 67–68, 475–484.
- Monteverdi, J.P., Doswell III, C.A., Lipari, G.S., 2003. Shear parameter thresholds for forecasting tornadic thunderstorms in northern and central California. *Weather Forecast.* 18, 357–370.
- Rasmussen, E.N., Blanchard, D.O., 1998. A baseline climatology of sounding-derived supercell and tornado forecast parameters. *Weather Forecast.* 13, 1148–1164.
- Setvák, M., Sálek, M., Munzar, J., 2003. Tornadoes within the Czech Republic: from early medieval chronicles to the “internet society”. *Atmos. Res.* 67–68, 589–605.
- Sioutas, M.V., 2003. Tornadoes and waterspouts in Greece. *Atmos. Res.* 67–68, 645–656.
- Snow, J.T. (Ed.), 2003. Proceedings of the European Conference on Severe Storms, Prague, 26–30 August 2002. *Atmos. Res.* 67–68, 703 pp.
- Snow, J.T., Dessens, J. (Eds.), 2001. Proceedings of the Conference on European Tornadoes and Severe Storms, Toulouse, 1–4 February 2000. *Atmos. Res.* 56. Elsevier, Ireland, 409 pp.
- Tyrell, J., 2003. A tornado climatology for Ireland. *Atmos. Res.* 67–68, 671–684.